

## SUPPLEMENTAL MATERIAL

### **Supplemental Methods:**

#### ***Plasmids and Antibodies***

The expression constructs for human *MOG1* (*pcDNA3-MOG1*) and human cardiac sodium channel gene *SCN5A* (*pcDNA3-SCN5A*) were obtained as described before.<sup>1</sup> Mutation G1743R in *hH1c1* and its wild-type control clones were generously provided by Jonathan C. Makielski.<sup>2</sup> The expression construct for the D1275N mutation in *pSP64* vector was kindly provided by Thomas Zimmer, and sub-cloned into *pcDNA3-SCN5A* (*AgeI*/ *BstEII*) to generate *pcDNA3-SCN5A/D1275N*. Polyclonal rabbit antibodies against *MOG1* and  $\text{Na}_v1.5$  were generated as previously described.<sup>1</sup> Mouse IgG directed against caveolin-3 was obtained from Santa Cruz Biotechnology, rabbit anti-GAPGH was from Cell Signaling Technology, and rabbit anti-N-Cadherin was from Novus Biologicals.

#### ***Isolation of Mouse Cardiomyocytes***

This study was approved by the Institutional Animal Care and Use Committee at the Cleveland Clinic. Mouse neonatal cardiomyocytes were isolated from 3-day-old CBA/B6 mouse neonates as previously described<sup>1</sup> using the Neonatal Rat/Mouse Cardiomyocyte Isolation kit (Cellutron Life Technology). The isolated myocytes were cultured for 2 days before transfection.

#### ***Cell Culture and Transfection***

A HEK293 cell line stably overexpressing  $\text{Na}_v1.5$  (HEK/ $\text{Na}_v1.5$ ) was a generous gift from Dr. Glenn E. Kirsch as previously described.<sup>1</sup> HEK/ $\text{Na}_v1.5$  cells were cultured in Dulbecco's

modified Eagle's medium (DMEM) supplemented with 10% fetal bovine serum, 2 mM glutamine, and penicillin-streptomycin. G418 (50  $\mu\text{g}/\mu\text{l}$ ) was added in the culture plate after splitting cells.

The HEK293 and tsA201 cells (a kind gift from Dr. Charles Antzelevitch) were maintained in Dulbecco's modified Eagle's medium (DMEM, Invitrogen) containing 10% (v/v) fetal bovine serum (FBS, Atlas Biological) at 37°C with 5% CO<sub>2</sub>. The expression constructs were transfected into the cells using Lipofectamine 2000 (Invitrogen) according to the manufacturer's instruction and incubated for 48 hrs before further analysis. For co-transfection in a 100 mm plate, 6.5  $\mu\text{g}$  of *pcDNA3-MOG1* or *pcDNA3* (vector control) and 3.1  $\mu\text{g}$  of wild type *pcDNA3-SCN5A* or each mutant *pcDNA3-SCN5A* construct were used.

### ***RNA Interference***

*MOG1*-specific small interfering RNAs (siRNAs) (designed using Dharmacon software) and control scrambler siRNAs (designed by GenScript) were synthesized by Dharmacon RNAi Technologies. Sequences of the siRNAs are shown in Supplemental Table 1. Blast analysis was used to confirm the specificity of the siRNAs for *MOG1* mRNA. All the siRNAs were conjugated with a green fluorochrome dye at their 5'-ends. The siRNAs were transfected into cells using oligofectamine (Invitrogen) and incubated for 48 hrs before further analysis.

### ***Isolation of Plasma Membranes (PM)***

Proteins on the PM were biotinylated at 4°C using EZ-Link Sulfo-NHS-SS-Biotin (Pierce). After quenching with ammonium chloride cells were lysed.<sup>3</sup> Equal amounts of cell lysates containing biotinylated proteins from each treatment group were incubated with UltraLink Immobilized NeutrAvidin Protein Plus beads (Pierce) to immobilize and precipitate the biotinylated proteins.

The precipitated biotinylated proteins from PM were eluted with SDS-PAGE sample buffer containing 50 mM DTT.

Alternatively, PM proteins were isolated by a centrifugation method as described elsewhere.<sup>4</sup> Briefly, cells were suspended in osmotic lysis buffer (25 mM Tris-HCl (pH 7.5), 5 mM EDTA, 5 mM EGTA and 1X protease inhibitor cocktail) and disrupted using Dounce homogenizer. Intact cells, nuclei and debris were removed by centrifugation at 1,000 X *g* for 5 min and clarified supernatant was centrifuged at 38,000 X *g* for 25 min at 4° C. The pellet containing membrane fractions was re-suspended in NP40 lysis buffer (1% v/v Nonidet P-40, 10% v/v glycerol, 137 mM NaCl, 20 mM Tris.HCl, pH 7.4, and 1X protease inhibitor cocktail) and used for subsequent analyses. Purity of the PM fraction prepared by this method was reported to be 95%.<sup>4</sup>

#### ***Assays for Stability of the PM Fraction of Na<sub>v</sub>1.5***

The assay was adapted from the endocytosis assay by Morimoto *et al.*<sup>3</sup> The cell surface proteins were biotinylated with 0.25 mg/mL Sulfo-NHS-SS-Biotin kit (Pierce) at 4° C for 30 min and quenched with 200 mM glycine at 4° C for 15 min. The cells were returned to the incubator to allow internalization to proceed. At specified time points, one set of the cells were subjected to biotin stripping from the cell surface with 50 mM MESNA (Sigma Aldrich) at 4° C for 30 min followed by quenching with 5 mg/mL iodoacetamide (Sigma Aldrich) at 4° C for 15 min. The cells from the biotin-stripped and the non-stripped sets were lysed in lysis buffer. The lysate from the biotin-stripped cells contained only the internalized biotinylated Na<sub>v</sub>1.5, while the lysate from the non-stripped cells contained the biotinylated Na<sub>v</sub>1.5 from both the PM and the internalized pool. Aliquots of an equal amount of total proteins were used to isolate the biotinylated proteins with UltraLink Immobilized NeutrAvidin Plus beads (Pierce). The abundance of biotinylated Na<sub>v</sub>1.5 was assessed by Western blot analysis using anti-Na<sub>v</sub>1.5 antibodies. The differential amount of biotinylated Na<sub>v</sub>1.5 between the biotin non-stripped and

stripped cells represents the amount of biotinylated-Na<sub>v</sub>1.5 that remains in the plasma membranes. The amount of plasma membrane Na<sub>v</sub>1.5 at each time point was used to calculate the percentage relative to time zero.

### ***Isolation of Rough Endoplasmic Reticulum (RER)-Enriched Fractions***

RER-enriched fractions were isolated by differential centrifugation using the Endoplasmic Reticulum Isolation Kit (Sigma) following the manufacturer's instruction. In brief, cells were pre-swollen in hypotonic buffer, homogenized and subjected to differential centrifugation at 4° C (1000 X g for 10min, 12,000 X g for 15 min) to remove nuclei, cell debris, mitochondria, and lipids. Then, this post mitochondrial fraction (PMF) was used for calcium chloride precipitation followed by a medium speed centrifugation (8,000 X g for 10 min) to obtain RER enriched fractions. The precipitated RER proteins were extracted with isotonic buffer and used for subsequent analyses.

### ***Fractionation of Caveolin-Enriched Membranes***

HEK/Na<sub>v</sub>1.5 cells were plated onto 100-mm culture dishes and transfected with a *caveolin-3-ECFP* plasmid by using Lipofectamin-2000 (Invitrogen). Experiments were conducted 2 days after transfection.

Caveolin-enriched fractions were prepared by using a detergent-free method described before with some modifications.<sup>5</sup> Briefly, cells were collected from the plates and centrifuged at 1,000 X g for 5 min. The cell pellet was resuspended in 2 ml of sodium carbonate solution (0.5 M, pH 11.0) and three 15 s homogenizing cycles were performed on ice. The homogenate was adjusted to 45% sucrose by addition of an equal volume of 90% sucrose in MBS (25 mM Mes, pH 6.5/ 0.15 M NaCl) and placed at the bottom of an ultracentrifuge tube. A 5-35%

discontinuous sucrose gradient was formed above by overlaying with 4 ml of 35% sucrose and then 4 ml of 5% sucrose. Tubes were centrifuged at 39,000 rpm for 18 hrs in an SW41 rotor. Twelve 1-ml fractions were collected from the top to the bottom of the gradient for subsequent Western blotting analysis.

### ***Western Blot (WB) Analysis***

WB was performed following standard protocols as previously described<sup>1</sup> using anti-Na<sub>v</sub>1.5 or anti-MOG1 antibodies at 1:500, and anti-GAPDH (Santa Cruz Biotechnology) or anti-N-Cadherin (Novus Biologicals) antibodies at 1:1000. Protein extracts were resolved by SDS-PAGE (8 to 10% as indicated in the figure legends), transferred to PVDF membranes and probed with respective antibodies. Membranes were washed and incubated with a HRP-conjugated corresponding secondary antibody and protein bands were detected using the ECL Detection Reagent (GE Healthcare). The intensity of each band on autoradiograms was analyzed by densitometry using the Melanie 2D Gel Analysis software trial version (Swiss Institute of Bioinformatics, Switzerland) and/or Quantity One 1D analysis software 4.6.3.Basic version (Bio-Rad Laboratories).

*For fractionations of caveolin-enriched membranes*, immunoblot analysis was carried out as described previously.<sup>5</sup> The density gradient fractions were denatured in a sample buffer, and heated at 37° C for 40 mins. Samples were electrophoresed on 10% SDS-polyacrylamide gels and transferred onto nitrocellulose membranes. The transferred blots were blocked with 5% non-fat milk in Tris-buffered saline and incubated for 1 h at room temperature with primary antibodies in TBS with 0.1% Tween 20. After washing, the blots were reacted with peroxidase-conjugated secondary antibodies for 45 min and developed using the ECL detection system (GE Healthcare).

### **Quantitative Real Time Reverse Transcription PCR (qRT-PCR) Analysis**

Total RNAs were isolated using TRIzol reagent (Invitrogen) and digested with DNase I (Applied Biosystems Inc). Reverse transcription of equal amounts of RNA was performed using the ImProm-II Reverse Transcription System (Promega Corporation). Quantitative real-time PCR was carried out using SYBR Green PCR Master Mix (Applied Biosystems Inc) with an ABI Prism 7900HT Sequence Detection System. All primer pairs (Supplemental Table 2) were optimized to ensure the specific amplification of the PCR products and the absence of primer dimerization. *GAPDH* and  *$\beta$ -Actin* were used as internal controls. Each run included a no-template control. Each sample was run in triplicates. The mRNA expression level was calculated as described by Chen *et al.*<sup>6,7</sup> Average changes in the relative mRNA expression of the target genes were used to generate the bar graphs.

### **Ionic Current Measurements**

The cardiac sodium current ( $I_{Na}$ ) was recorded from neonatal cardiomyocytes transfected with *MOG1*/scrambler siRNAs as well as from HEK/Na<sub>v</sub>1.5 cells and tsA201 cells transfected with *SCN5A/MOG1* expression plasmids following the protocol described earlier by us.<sup>1</sup> In brief, experiments were conducted using a MultiClamp 700A amplifier interfaced to a Pentium computer equipped with Digidata 1322A and pClamp9 software (Axon Instruments). Pipettes were fabricated from borosilicate glass capillaries (FHC) and fire-polished with 1.5-2.0 M $\Omega$  resistance (seal resistance was 2-3 G $\Omega$ ). Whole-cell membrane capacitances and series resistances were 85% compensated electronically. Sodium currents were elicited by depolarizing pulses from -100 mV to + 70 mV in HEK/Na<sub>v</sub>1.5 cells and tsA201 cells.  $I_{Na}$  was elicited and recorded using a single pulse from -100 mV to -20 mV in neonatal cardiomyocytes.  $I_{Na}$  was recorded by holding cells at -100 mV and depolarizing in 5 mV increments. Currents

were filtered at 5 kHz (-3 dB, 4-pole Bessel filter) following series resistance compensation. For  $I_{Na}$  current recordings, the composition of pipette solution was (in mmol/L): 20 NaCl, 150 CsCl, 10 HEPES and 10 EGTA, pH 7.2 (adjusted with CsOH). The holding potential for all pulse protocols was -100 mV, and experiments were performed at room temperature (22° C). For HEK/Na<sub>v</sub>1.5 cells and tsA201 cells, the composition of the bath solution was as follows (in mmol/L): 70 NaCl, 80 CsCl, 5.4 KCl, 2 CaCl<sub>2</sub>, 1 MgCl<sub>2</sub>, 10 HEPES and 10 glucose, pH 7.3 (adjusted with CsOH). For neonatal cardiomyocytes, the NaCl concentration was reduced to 20 mM, and CsCl was increased to 120 mM for better voltage control. To eliminate the contamination of L-type calcium current and transient outward potassium current, 2 mM CdCl<sub>2</sub> and 2 mM 4-aminopyridine were added to the bath solution, respectively. The membrane potential dependence of inactivation was estimated using two-pulse protocol. Data for the voltage dependence of activation and inactivation were fitted with the Boltzmann equation. A two-pulse protocol was used to measure the recovery rate from inactivation with the fractional current (P2/P1) plotted against inter-pulse duration between P1 and P2, and the fraction of channels recovered at various time intervals was quantified by dividing the peak current measured during a test pulse to -20 mV. The mean maximum conductance values were calculated as described previously.<sup>8</sup>

The late sodium current ( $I_{NaL}$ ) was elicited using a single pulse from -100 to -20 mV for 775 ms. The  $I_{NaL}$  amplitude was measured as the averaged current within 200-220 ms and normalized to the peak  $I_{Na}$ .

The L-type calcium current ( $I_{Ca-L}$ ) and the transient outward potassium current ( $I_{To}$ ) were recorded from neonatal cardiomyocytes transfected with *MOG1* si-RNAs or scrambler siRNAs. Following a protocol by Rizzi *et al*,<sup>9</sup> we recorded  $I_{Ca-L}$  with 200 ms depolarizing pulses from a holding potential of -40 mV, with 10 mV steps from -40 mV to -60 mV. The pipette solution filled with buffer with the following composition (in mmol/L): 80 Aspartate acid, 10 NaCl, 2 MgCl<sub>2</sub>, 70 CsOH, 40 CsCl, 10 EGTA, 2 Na<sub>2</sub>ATP, 0.1 GTP and 10 HEPES (pH adjusted to 7.2 with CsOH).

The bath solution contained (in mmol/L): 140 NaCl, 4 CsCl, 1 CaCl<sub>2</sub>, 1 MgCl<sub>2</sub>, 10 HEPES, 5 glucose and 0.02 tetrodotoxin (pH adjusted to 7.4 with NaOH).

For recordings of the  $I_{T_o}$  current, the cells were held at a potential of -60 mV to inactivate  $I_{Na}$  and depolarized with 800 ms step pulses in 10 mV increments to +60 mV at 3s intervals. Pipette resistance was 2-3 M $\Omega$  when filled with buffer with the following composition (in mmol/L): 20 KCl, 110 K-aspartate, 5 HEPES, 5 EGTA, 2 MgCl<sub>2</sub>, 5 K<sub>2</sub>ATP and 5 Na<sub>2</sub>-Phosphocreatine, pH 7.2 with KOH. External buffer consisted of (in mM): 130 N-methyl-D-glucamine, 5.4 KCl, 1.2 MgSO<sub>4</sub>, 10 HEPES and 10 glucose, pH 7.4 (adjusted with HCl). Nifedipine at 3  $\mu$ M was added to block the L-type calcium channel.



**Supplemental Tables:**

**Table 1:** Sequences of the siRNAs used to knock *MOG1* expression down

siRNA	Sequence
siRNA1	5'-GAGCCTGAGTAACTTTGAA-3'
siRNA2	5'-GTGCGTAAACATAAGACAA-3'
scrambler1	5'-TCATGCCATTCTTAGTAAT-3'
scrambler2	5'-CGATAGATTCTAGACTGGA-3'

**Table 2:** Sequences of the primers used for quantitative real time RT-PCR analysis

Genes	Primers	Human	Mouse
<i>MOG1</i>	F	5'-ATG GAG CCC ACG AGA GAC T-3'	5'-TAT CCC TGA GAG GCT GCT G-3'
	R	5'-ACT CCA CAT GGA CAG CCC TA-3'	5'-TCC AAG GTG GAC ATG ACA G-3'
<i>SCN5A</i>	F	5'-ATT CTG GTT CAC TCG CTC TTC-3'	5'-CCT CCA AAA AGC TGC CAG-3'
	R	5'-CTT GAC CAG AGA CTC AAA GGT GT-3'	5'-CAT TGG TGG CAC TGA ACC-3'
<i>SLC25A35</i>	F	5'-CCC ATC TAC ATG GTG AAG AC-3'	5'-GGT CAT GGG AGC ATA TCT GG-3'
	R	5'-GAG GAA AGA TCT CCC ACT G-3'	5'-GGT AGA GGA GCC GAT GAC-3'
<i>GAPDH</i>	F	5'-CAA AGT TGT CAT GGA TGA CC-3'	5'-AGG TCG GTG TGA ACG GAT TTG-3'
	R	5'-CCA TGG AGA AGG CTG GGG-3'	5'-TGT AGA CCA TGT AGT TGA GGT CA-3'
<i>β Actin</i>	F	5'-CCT GGC ACC CAG CAC AAT-3'	5'-GGT CAT CAC TAT TGG CAA CG-3'
	R	5'-GCC GAT CCA CAC ACG GAG TAC T-3'	5'-ACG GAT GTC AAC GTC ACA CT-3'

**Table 3:** Biophysical parameters of WT sodium channels in the presence/absence of siRNA against *MOG1*

	Peak Current Density		Steady-State Activation		Steady-State Inactivation		Recovery From Inactivation	
	pA/pF	n	V <sub>1/2</sub> (mV)	n	V <sub>1/2</sub> (mV)	n	T1 (ms)	n
<b>siRNA1</b>	-60.76 ± 11.45*	6	-46.32 ± 0.41	6	-83.44 ± 0.24	6	7.13 ± 0.23	6
<b>scrambler1</b>	-122.53 ± 22.55	5	-49.29 ± 0.25	5	-81.79 ± 0.17	5	7.56 ± 0.25	5
<b>siRNA2</b>	-69.34 ± 15.59*	6	-47.32 ± 0.35	6	-88.20 ± 0.20	6	7.02 ± 0.18	6
<b>scrambler2</b>	-163.56 ± 32.55	6	-51.06 ± 0.23	6	-86.28 ± 0.31	6	7.45 ± 0.27	6

\**P* < 0.05 compared to corresponding scrambler**Table 4:** Biophysical parameters of WT and D1275N mutant channels in the presence/absence of *MOG1*

	Peak Current Density		Steady-State Activation			Steady-State Inactivation			Recovery From Inactivation	
	pA/pF	n	V <sub>1/2</sub> (mV)	K (mV)	n	V <sub>1/2</sub> (mV)	K (mV)	n	T1 (ms)	n
<b>WT - MOG1</b>	-139.00 ± 13.80	10	-42.00 ± 1.32	5.56 ± 0.44	10	-90.27 ± 1.71	4.51 ± 0.24	10	14.66 ± 0.66	10
<b>WT + MOG1</b>	-185.89 ± 18.30*	10	-40.54 ± 1.97	6.05 ± 0.10	10	-87.68 ± 2.42	4.56 ± 0.08	10	16.35 ± 0.78	10
<b>D1275N - MOG1</b>	-92.44 ± 12.93*	10	-32.15 ± 1.26*	7.65 ± 0.80	10	-77.69 ± 1.60*	4.39 ± 0.20	10	7.04 ± 0.23	10
<b>D1275N + MOG1</b>	-181.44 ± 9.78*	10	-30.38 ± 1.86*	5.45 ± 0.55	10	-78.63 ± 1.00*	4.73 ± 0.06	10	10.53 ± 0.27	10

\**P* < 0.05 compared to (WT - MOG1)

**Table 5:** Biophysical parameters of WT and (G1743R+WT) channels in the presence/absence of *MOG1*

	Peak Current Density		Steady-State Activation			Steady-State Inactivation			Recovery From Inactivation	
	pA/pF	n	V <sub>1/2</sub> (mV)	K (mV)	n	V <sub>1/2</sub> (mV)	K (mV)	n	T1 (ms)	n
<b>WT - MOG1</b>	-56.56 ± 8.00	7	-43.95 ± 0.91	5.89 ± 0.49	7	-88.37 ± 0.85	4.91 ± 0.25	7	14.21 ± 0.12	7
<b>WT + MOG1</b>	-110.56 ± 7.80*	7	-40.07 ± 0.98	5.51 ± 0.23	7	-85.78 ± 0.62	4.35 ± 0.12	7	16.07 ± 0.34	7
<b>(G1743R+WT) - MOG1</b>	-31.98 ± 5.33*	7	-44.32 ± 1.37	6.41 ± 0.67	7	-87.49 ± 2.44	4.75 ± 0.75	7	15.69 ± 0.33	7
<b>(G1743R+WT) + MOG1</b>	-50.33 ± 9.55	7	-42.49 ± 1.42	5.85 ± 0.71	7	-86.87 ± 1.33	4.45 ± 0.34	7	15.28 ± 0.27	7

\**P* < 0.05 compared to (WT - MOG1)

**Supplemental Figure Legends:**

**Figure S1. Knockdown of *MOG1* expression by the second *MOG1* siRNA (siRNA2) reduced  $I_{Na}$  density in HEK/Na<sub>v</sub>1.5 cells.** **A.** Raw traces of a family of sodium currents in HEK/Na<sub>v</sub>1.5 cells transfected with scrambler siRNA (scrm, Left) or *MOG1* specific siRNA2 (Right) elicited by depolarizing pulses from -100 mV to +70 mV. **B.** Effects of siRNA2 on the current-voltage relationship of Na<sub>v</sub>1.5.  $I_{Na}$  was recorded by holding cells at -100 mV and depolarizing in 5 mV increments. The current amplitudes were normalized to cell capacitance (pA/pF, abscissa). Compared to scrm, siRNA2 markedly reduced  $I_{Na}$  density. **C.** Effects of siRNA2 on steady-state activation (Right) and inactivation (Left) of Na<sub>v</sub>1.5. The membrane potential dependence of inactivation was estimated using two-pulse protocols (see inset). There were no detectable changes in activation or inactivation in siRNA2 versus scrm -treated cells. **D.** Effects of siRNA2 on recovery from inactivation of Na<sub>v</sub>1.5. A two-pulse protocol was used to measure the recovery rate from inactivation with the fractional current (P2/P1) plotted against inter-pulse duration between P1 and P2, and the fraction of channels recovered at various time intervals was quantified by dividing the peak current measured during a test pulse to -20 mV. Recovery of sodium channel inactivation was unaffected by siRNA2.

**Figure S2. Knockdown of *MOG1* expression by *MOG1* siRNA1 and siRNA2 led to significantly decreased peak  $I_{Na}$  densities in HEK293/Na<sub>v</sub>1.5 cells compared to scrambler siRNAs (scrm1 and scrm2).**

**Figure S3. Overexpression of *MOG1* did not affect late sodium currents by Na<sub>v</sub>1.5 in tsA201 cells.** **A.** Raw traces of sodium current ( $I_{Na}$ ).  $I_{Na}$  was elicited using a single pulse from -100 to -20 mV for 775 ms. The peak  $I_{Na}$  was off-scale for better illustration of the late  $I_{Na}$ . tsA201 cells were co-transfected with a *SCN5A* expression plasmid and a expression plasmid

for *MOG1* (+*MOG1*) or empty vector (control, -*MOG1*). **B.** The ratio of the late  $I_{Na}$  over the peak  $I_{Na}$  is shown. The late  $I_{Na}$  amplitude was measured as the averaged current within 200-220 ms and normalized to the peak  $I_{Na}$ . Note that the  $\Delta$ KPQ mutation markedly increased the late sodium current, and *MOG1* did not affect the late sodium current generated by either wild type or mutant  $Na_v1.5$ .

**Figure S4. Knockdown of *MOG1* expression by the second siRNA (siRNA2) markedly reduced  $I_{Na}$  densities in neonatal cardiomyocytes.** **A.** Relative mRNA levels of *MOG1* were analyzed by qRT-PCR analysis. Transfection of *MOG1* specific siRNA2 to mouse neonatal cardiomyocytes decreased the amount of *MOG1* mRNA significantly. **B.** Raw traces of peak  $I_{Na}$  and current densities.  $I_{Na}$  was elicited and recorded using a single pulse from -100 mV to -20 mV. The peak  $I_{Na}$  was expressed as current densities (pA/pF, current amplitudes normalized to cell capacitance) and averaged for the cell group (n=13 for scrm and n=7 for siRNA2). Current densities were  $10.15 \pm 3.28$  (si-RNA2) and  $117.99 \pm 11.73$  pF (scrm); \*,  $P=4.93 \times 10^{-5}$ .

**Figure S5. Knockdown of *MOG1* expression did not affect the density of L-type calcium current ( $I_{Ca-L}$ ) in neonatal cardiomyocytes.** **A-D.** Typical raw traces of  $I_{Ca-L}$  in neonatal cardiomyocytes transfected with scramble siRNA1 (scrm1) (**A**), siRNA1 against *MOG1* (**B**), scrm2 (**C**), or *MOG1* siRNA2 (**D**). **E.** The current detected in neonatal cardiomyocytes was nifedipine-sensitive  $I_{Ca-L}$ . **F.** Mean current-voltage relationship of  $I_{Ca-L}$  recorded from neonatal cardiomyocytes transfected with scrm1 or siRNA1. **G.** Mean current-voltage relationship of  $I_{Ca-L}$  from neonatal cardiomyocytes transfected with scrm2 or siRNA2.

**Figure S6. Knockdown of *MOG1* expression did not affect the density of the  $I_{To}$  potassium current in neonatal cardiomyocytes.** **A-D.** Representative raw traces of  $I_{To}$  recorded from neonatal cardiomyocytes transfected with scramble siRNA1 (scrm1) (**A**), *MOG1*-

specific siRNA1 (B), scrm2 (C), or *MOG1* siRNA2 (D). E. Mean current-voltage relationship of  $I_{T0}$  recorded from neonatal cardiomyocytes transfected with scrm1 or siRNA1. F. Mean current-voltage relationship of  $I_{T0}$  recorded from neonatal cardiomyocytes transfected with scrm2 or siRNA2.

**Figure S7. *MOG1* can be detected in the RER-enriched fraction from HEK/Na<sub>v</sub>1.5 cells.** *pcMOG1* (OverExp) and *siMOG1* (siRNA) increased and decreased the amount of *MOG1* in the RER fractions compared to that from control cells (Control), respectively. Total protein lysates from *pcMOG1*-transfected cells (OverExp) were used as positive control. Calnexin WB served as a loading control.

**Figure S8. *MOG1* overexpression fully rescued the reduced peak  $I_{Na}$  by D1275N trafficking defective mutant Na<sub>v</sub>1.5.** The tsA201 cells were co-transfected with a WT or mutant D1275N Na<sub>v</sub>1.5 expression plasmid and *MOG1* expression plasmid (+*MOG1*) or empty vector (control, -*MOG1*).  $I_{Na}$  was recorded as described in the Methods section. The peak  $I_{Na}$  densities (pA/pF) were plotted. D1275N mutant channels showed significantly lower peak  $I_{Na}$  density compared to wild type channels. In the presence of *MOG1*, no significant difference of the peak  $I_{Na}$  density was detected between mutant and wild type channels, indicating that *MOG1* fully restored the function of D1275N mutant channels.

**Figure S9. *MOG1* overexpression rescued the reduced peak  $I_{Na}$  by G1743R trafficking defective mutant Na<sub>v</sub>1.5 to the WT level at a heterozygous state (mixed WT and G1743R).** The tsA201 cells were co-transfected with a WT or mutant G1743R Na<sub>v</sub>1.5 expression plasmid and *MOG1* expression plasmid (+*MOG1*) or empty vector (control, -*MOG1*).  $I_{Na}$  was recorded as described in the Methods section. The peak  $I_{Na}$  densities (pA/pF) were plotted. Since the G1743R mutation completely eliminated  $I_{Na}$ , we analyzed the effect of mutation G1743R by co-

transfecting tsA201 cells with an equal amount of WT and G1743R Na<sub>v</sub>1.5 expression constructs, which mimicks the heterozygous state in BrS patients. The peak  $I_{Na}$  density for mixed G1743R+WT channels in the presence of MOG1 was similar to WT channels, demonstrating that overexpression of MOG1 can restore the level of peak  $I_{Na}$  densities in the heterozygous state (G1743R+WT) to that of homozygous wild-type state.

**Figure S10. MOG1 does not affect the PM expression of Kir2.1 in tsA201 cells.** Relative amounts of Kir2.1 on the PM of tsA201 cells were analyzed by WB analysis (12% gel, Top) and quantified by densitometry (Bottom). N-cadherin was used as loading control for PM proteins. **A.** Cells transfected with siRNA for MOG1 failed to show any significant change in Kir2.1 protein expression on the PM compared to that from cells transfected with scrm. **B.** No significant difference was observed for PM Kir2.1 expression in cells overexpressing MOG1 compared to vector-control cells.

**Supplemental Figures**

**Figure S1.**

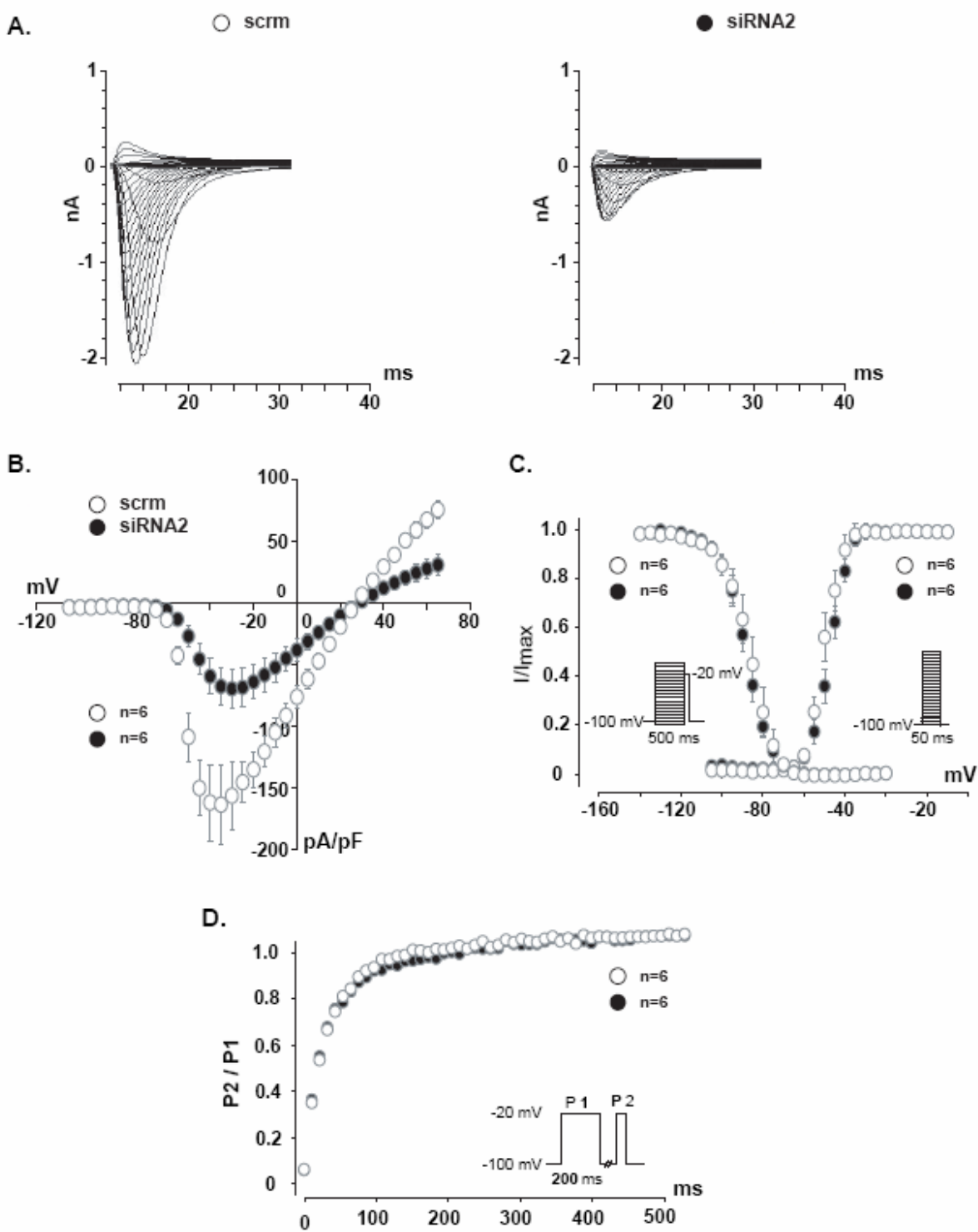




Figure S2.

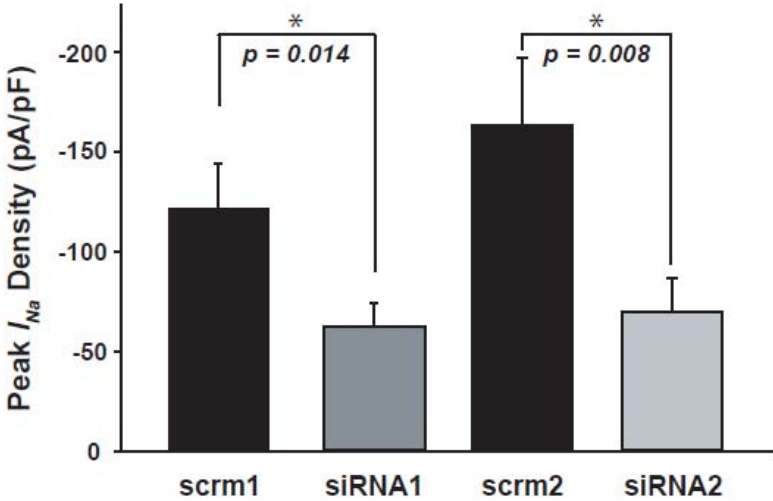
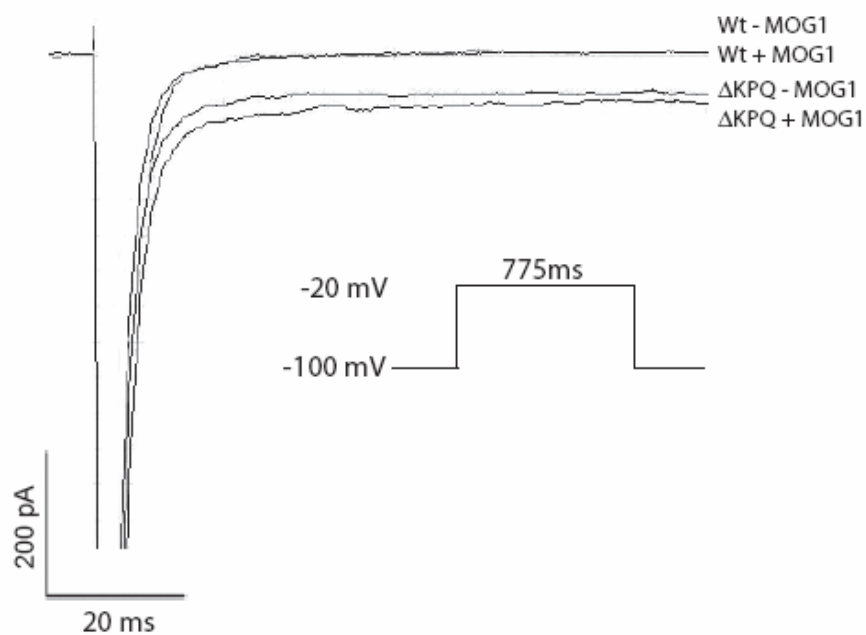


Figure S3.

A.



B.

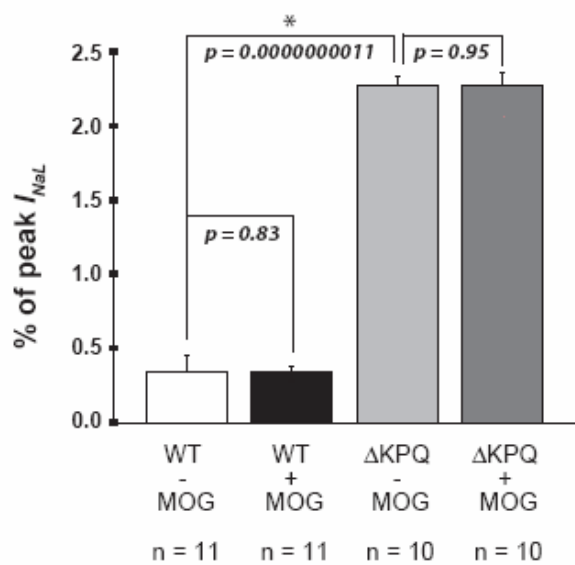
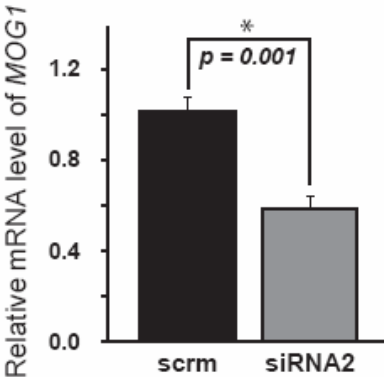


Figure S4.

A.



B.

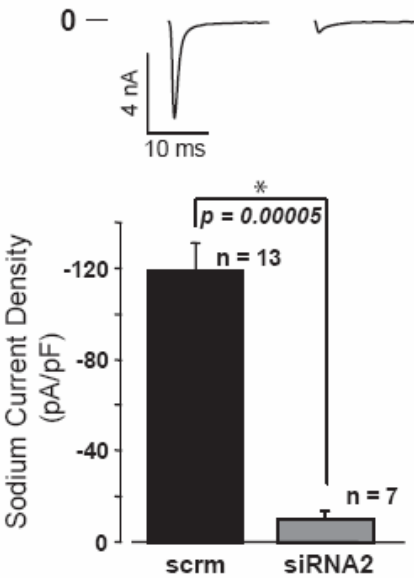


Figure S5.

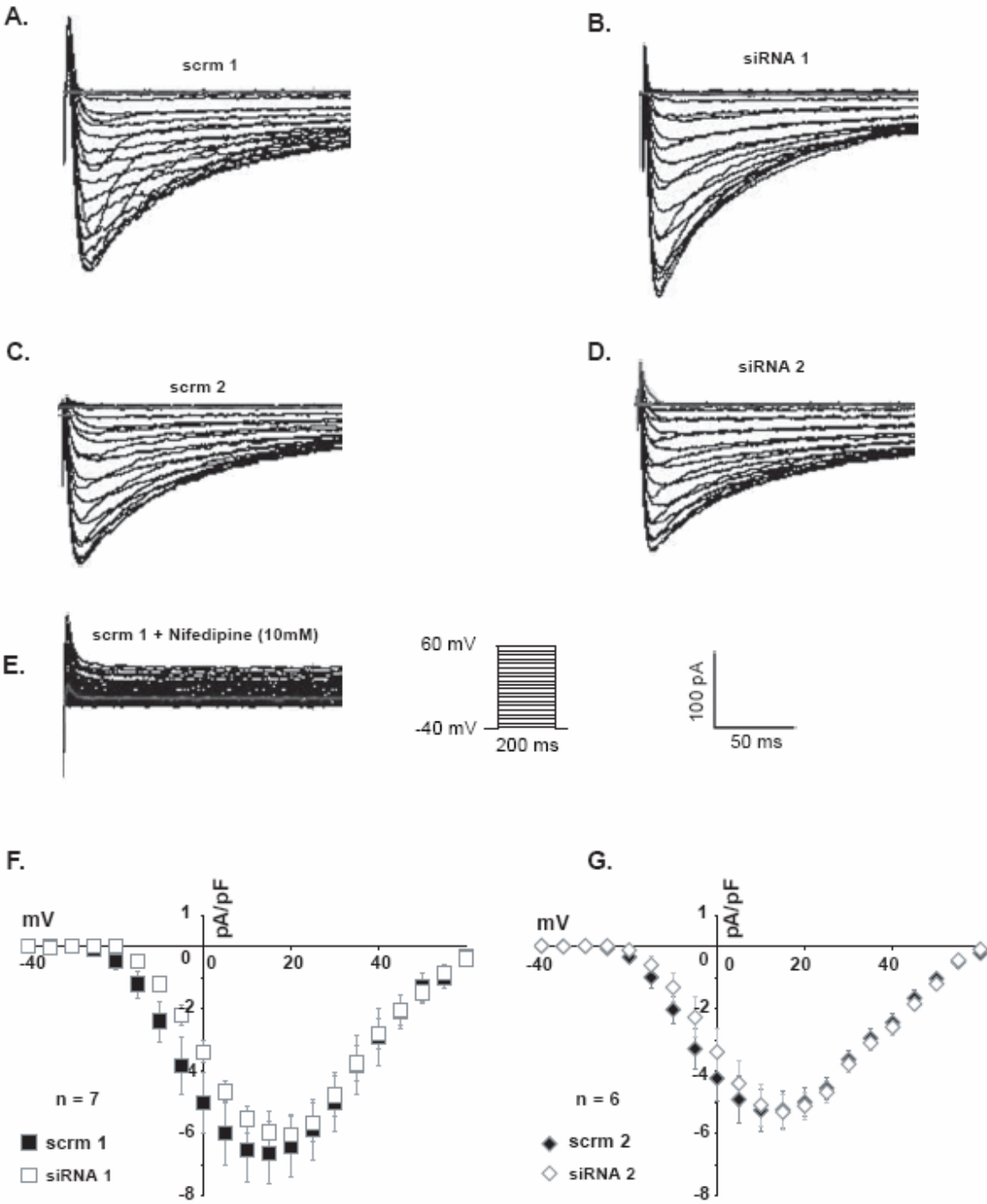
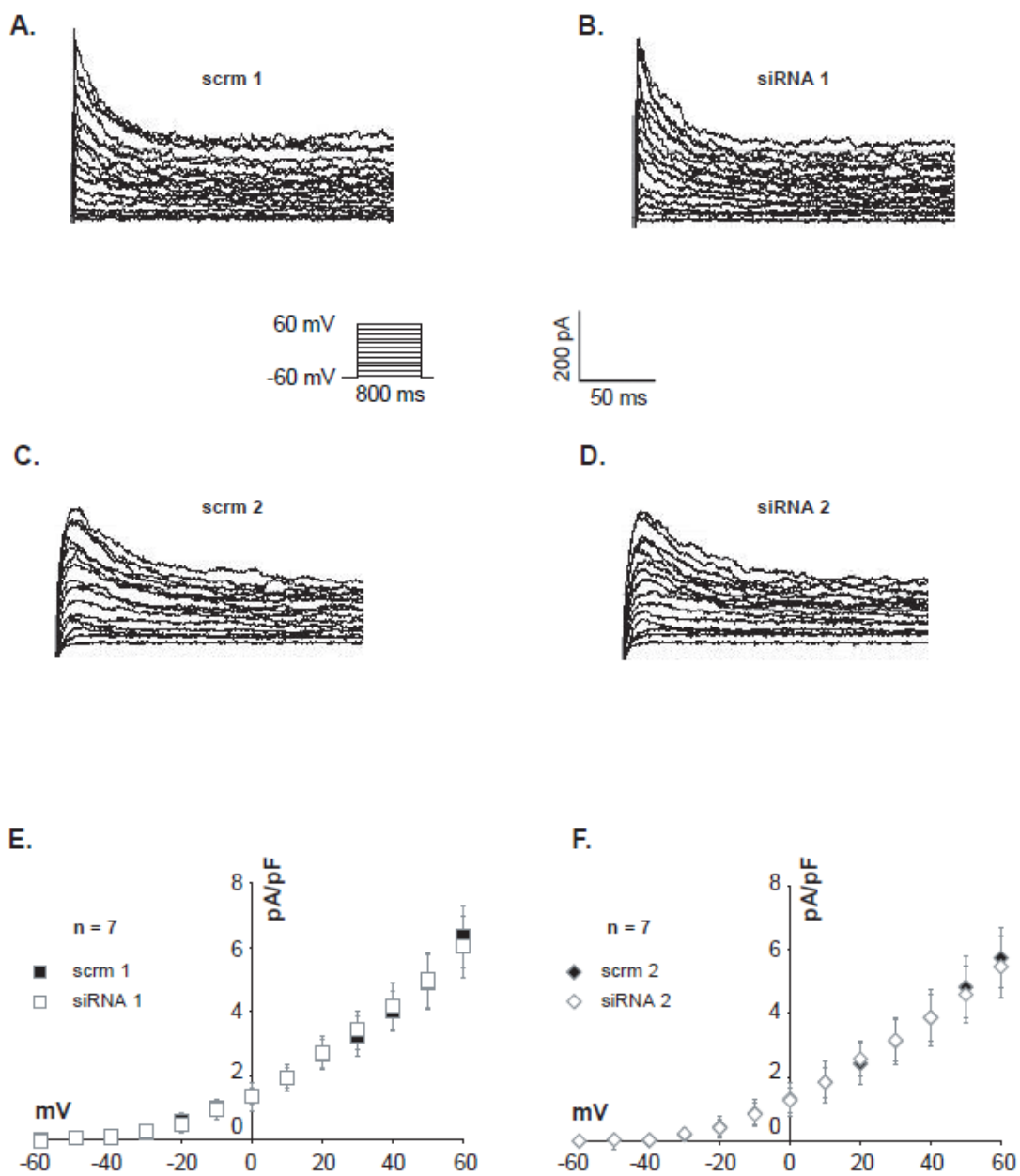


Figure S6.



**Figure S7.**

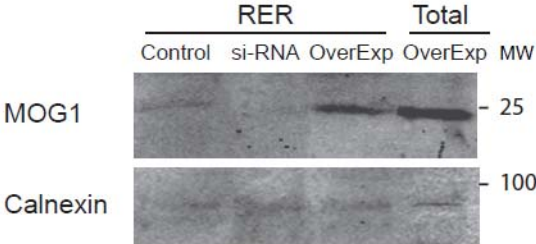


Figure S8.

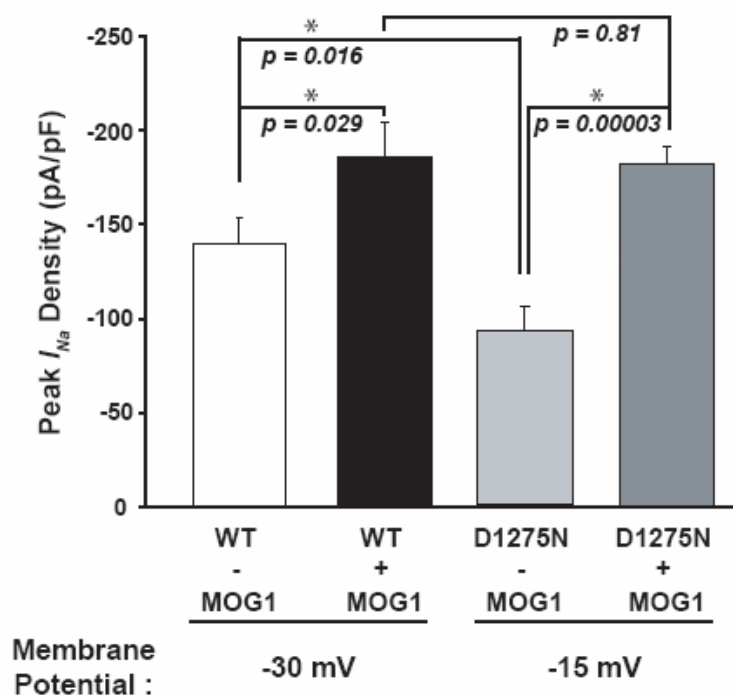


Figure S9.

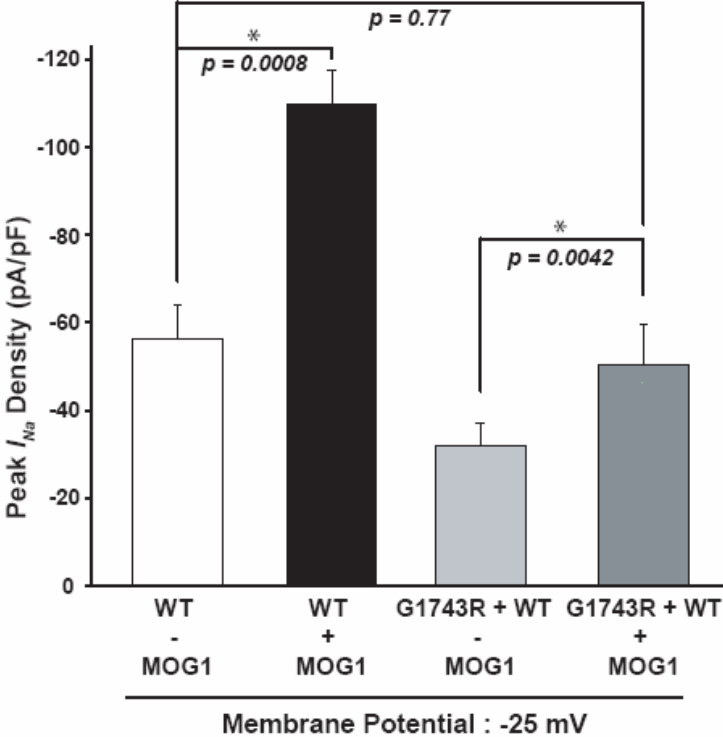
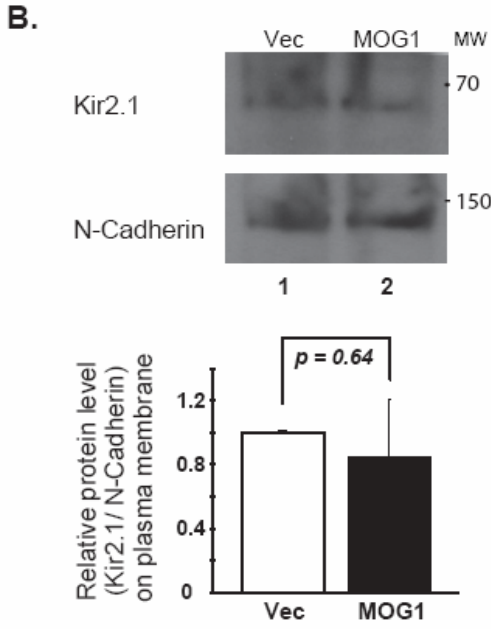
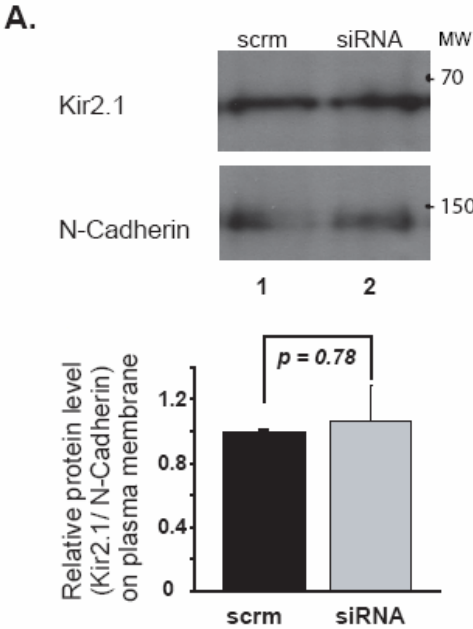




Figure S10.



### **Supplemental References:**

1. Wu L, Yong SL, Fan C, Ni Y, Yoo S, Zhang T, Zhang X, Obejero-Paz CA, Rho HJ, Ke T, Szafranski P, Jones SW, Chen Q, Wang QK. Identification of a new co-factor, MOG1, required for the full function of cardiac sodium channel Nav 1.5. *J Biol Chem.* 2008;283:6968-6978.
2. Valdivia CR, Tester DJ, Rok BA, Porter CB, Munger TM, Jahangir A, Makielski JC, Ackerman MJ. A trafficking defective, Brugada syndrome-causing SCN5A mutation rescued by drugs. *Cardiovasc Res.* 2004;62:53-62.
3. Morimoto S, Nishimura N, Terai T, Manabe S, Yamamoto Y, Shinahara W, Miyake H, Tashiro S, Shimada M, Sasaki T. Rab13 mediates the continuous endocytic recycling of occludin to the cell surface. *J Biol Chem.* 2005;280:2220-2228.
4. Naga Prasad SV, Barak LS, Rapacciuolo A, Caron MG, Rockman HA. Agonist-dependent recruitment of phosphoinositide 3-kinase to the membrane by beta-adrenergic receptor kinase 1. A role in receptor sequestration. *J Biol Chem.* 2001;276:18953-18959.
5. Garg V, Jiao J, Hu K. Regulation of ATP-sensitive K<sup>+</sup> channels by caveolin-enriched microdomains in cardiac myocytes. *Cardiovasc Res.* 2009;82:51-58.
6. Chen Q, Zhang T, Roshetsky JF, Ouyang Z, Essers J, Fan C, Wang Q, Hinek A, Plow EF, Dicorleto PE. Fibulin-4 regulates expression of the tropoelastin gene and consequent elastic-fibre formation by human fibroblasts. *Biochem J.* 2009;423:79-89.
7. Zhang X, Chen S, Yoo S, Chakrabarti S, Zhang T, Ke T, Oberti C, Yong SL, Fang F, Li L, de la Fuente R, Wang L, Chen Q, Wang QK. Mutation in nuclear pore component NUP155 leads to atrial fibrillation and early sudden cardiac death. *Cell.* 2008;135:1017-1027.

8. Bendahhou S, Cummins TR, Tawil R, Waxman SG, Ptacek LJ. Activation and inactivation of the voltage-gated sodium channel: role of segment S5 revealed by a novel hyperkalaemic periodic paralysis mutation. *J Neurosci*. 1999;19:4762-4771.
9. Rizzi N, Liu N, Napolitano C, Nori A, Turcato F, Colombi B, Bicciato S, Arcelli D, Spedito A, Scelsi M, Villani L, Esposito G, Boncompagni S, Protasi F, Volpe P, Priori SG. Unexpected structural and functional consequences of the R33Q homozygous mutation in cardiac calsequestrin: a complex arrhythmogenic cascade in a knock in mouse model. *Circ Res*. 2008;103:298-306.